Determining the origin of volcanic rocks in the mélange complex of Karangsambung based on the electrical resistivity imaging

Lina Handayani[1*], Ilham Arisbaya[1], M. Maruf Mukti[1], Yayat Sudrajat[1]

[1] Research Center for Geotechnology, Indonesian Institute of Sciences

* Corresponding author. E-mail address: lina.handayani@gmail.com,

ABSTRACT

An ENE-WSW-trending localized basalt-diabase outcrop along the SE margin of Luk Ulo Mélange Complex has been suggested as intrusive rocks cut through the Paleogene Totogan and Karangsambung formations. However, the absolute dating of the volcanics is older than the inferred relative age of the sedimentary formations, hence the in-situ intrusion theory is less likely. A subsurface imaging should delineate the possibility of the in-situ nature of volcanic rock by looking at the continuation of the rocks to the depth. In this study, we did a subsurface imaging by electrical resistivity method. The electrical resistivity surveys were conducted at 3 (three) lines across the ENE-WSW trend of the volcanic distribution. From those three measurements, we obtained three inversion models that present the distribution of the resistivity. We could differentiate between the high resistivity of volcanic rocks and the low resistivity of the clay-dominated sediments. Instead of the deep-rooted intrusions, the geometry of the volcanic rocks is concordant with the sedimentary strata. Since we do not observe any spatial continuity of the bodies, both laterally and vertically, the volcanic rocks might be part of broken intrusive rocks. Furthermore, the size and the sporadically distributed of the rocks also indicated that they are more likely as fragments during the olistostrome deposition, transported from its original location.

Keywords: mélange complex, olistostrome, volcanic rocks, electrical resistivity, Karangsambung

1. INTRODUCTION

Understanding the subsurface geometry of volcanic-plutonic bodies is crucial for better understanding the eruption history and processes afterwards, especially in a tropical active margin region where the interplay between climate that enhances weathering, erosion of rock exposures, and tectonic activity that deforming the rock formations occurred. With the application of geophysical modeling, it is possible to image the subsurface architecture of the volcanic-plutonic conduits system (Blaikie et al., 1988; Ogawa et al., 1998). However, the application of such methods in the region that underwent intense and multiple tectonic phases is challenging. In the Karangsambung area, Central Java, a vast exposure of various rocks with different origins exhibited as a mélange complex. A volcanic unit, which consists of plutonic – andesitic basalt and diabase, is scattered with a trend of ENE-WSW within the olistostrome and deep marine deposits of Karangsambung and Totogan Formations (Figure 1). This unit is called the Dakah volcanic unit (Yuwono, 1997), and the primary outcrop is basalt-diabase in Dakah and Mount Parang. The volcanic apparently cut through the Karangsambung and Totogan Formation (Prasetyadi et al., 2005; Harsolumakso, 1996; Soeria-Atmadja et al., 1994; Asikin, 1974). Usually, the volcanic intrusion's nature implies that the volcanic source was directly beneath those formations, and the age of the volcanic is younger than the sedimentary environments. However, since the formations are olistostromal products, there is a possibility that those basalt-diabase rocks had been transported from its original location, particularly when there is a doubt in age reconstruction (Soeria-Atmadja et al., 1994).

There are currently two groups of opinions that explained the presence of these volcanic in Karangsambung and Totogan Formations. The first group suggested that the basalts are volcanic fragments deformed during the generation of olistostrome, along with the rest of the sedimentary formations. This suggestion was based on the abundance of basaltic elements within the sedimentary matrix (Harsolumakso, 1999; Asikin, 1974). The deformation of gravity sliding that caused the olistostrome occurred after the sediment and volcanic product deposition. The second group explained that the volcanism occurred in-situ due to the basalts' scattered pattern and their bearing within the sediment formations (Setiawan et al., 2011; Prasetyadi et al., 2006; Yuwono, 1997). The exposed diabase at Mount Parang and Dakah is also a columnar joint associated with an intrusion or a volcanic neck. Geochemical analysis of the Dakah volcanic unit has indicated that all types of volcanic rock from this area have a similar magma origin, which is from sub-marine volcanism of an island arc (Setiawan et al., 2011). Further evaluation of magma evolution and exposed basaltic distribution suggest that the Dakah village was a center of Late Eocene-Oligocene volcanic activities (Setiawan et al., 2011). For the second theory, the volcanic existed after the process of deformation. Therefore, the center of the volcanic activity should be located within the area of current basaltic distribution.

All previous geological reports on the Dakah volcanic origin were based on the exposed rocks and the age determination. Subsurface observation might benefit in determining the depth of the continuation of volcanic rock, which is important in analyzing the volcanic origin. However, probably due to the region's complexity, very few geophysical studies have ever been applied in this area. A regional study of seismic tomography presented a moderate seismic velocity at the central Java and interpreted as a trace of mélange assemblages (Haberland et al., 2014). A gravity model suggested that basaltic in Mount Parang is a segment of an intrusion (Kamtono, 1995). He described an igneous body of intrusion cut through the higher densities environment, which is associated with the tectonic mélange complex. Later, Laesanpura (Laesanpura et al., 2017) applied the 1-D Audio-magnetotellurics (AMT) at 3 (three) stations. The three 1D inversion models did not show any continuity in the subsurface layers. However, the model at Mount Parang presented a high resistivity layer associated with diabase at a depth of between 100 and 400 meters. The body of diabase appeared as a floating body above the sediment formation. Therefore, they concluded that the volcanic unit at Mount Parang as a sill.

This study aims to find the continuity to the depth of the basalt-diabase in Karangsambung by subsurface imaging. The subsurface investigation might difficult in such a mélange complex. The nature of most rocks in the area is 'block-in-matrix' types. Any measurement of physical properties might give average values of the rock fragments and the matrix combined. Therefore, we concentrated on finding the largest volcanic rock block to estimate the distribution to the depth. For this purpose, we applied the electrical resistivity imaging. The method has been efficiently used in (Junaid et al., 2019) for the subsurface investigation to find granite boulders. Previous researches have used it for volcanic body investigations (Barde-cabusson et al., 2013; Ingham, 2005; Troiano et al., 2019). They used the electrical resistivity tomography in active volcanoes and provided the subsurface information that could not be established with a regular surface geological survey. Although each type of rock has quite wide-ranging resistivity values, the electrical resistivity method can sufficiently detect the difference between hard (i.e., igneous/volcanic/metamorphic) and soft (i.e., sediments) rocks to the wide variation in their conductivity properties.

2. GEOLOGICAL SETTINGS

Karangsambung region, Central Java, is a complex of various rocks and formations generated by different tectonic processes. Due to the extent of variations, the geological properties of the area are considered the key to understanding the evolution of Java Island and Southeast Asia in general (Figure 1A). The Karangsambung mélange complex comprises tectonic mélange and olistostrome mélange (Wakita, 2000; Suparka, 1988; Asikin, 1974). The tectonic mélange was formed in Cretaceous time and consisted of various rock fragments in a scaly clay matrix, which indicates a subduction accretionary related process (Suparka, 1988; Asikin, 1974).

The tectonic mélange in Karangsambung includes dismembered ophiolite, volcanic rocks, metamorphic rocks, and sedimentary rocks (e.g., Wakita, 2000; Asikin et al., 1992; Suparka, 1988; Asikin, 1974) (Figure 1B). The ophiolites consist of serpentinized harzburgite, serpentinite, lherzolite, gabbro, diabase, and pillow basalt, with some of them are of mid-oceanic ridge origin from 81-85 Ma (Suparka, 1988). The metamorphic unit comprises high-pressure (HP) metamorphic rocks such as eclogite, glaucophane, and blueschist, medium pressure rocks that include garnet amphibolite and greenschist, and ordinary crystalline schists and gneisses (Kadarusman et al. 2007; Miyazaki et al. 1998; Parkinson et al. 1998). Fragments of some HP metamorphic rocks formed small tectonic blocks in sheared serpentinite along fault zones, whereas some amphibolite-facies schists are found structurally intercalated within sedimentary blocks (Kadarusman et al. 2007). The radiolarian data from the sedimentary rocks indicates Early - Late Cretaceous of deposition and middle to latest Cretaceous or earliest Paleocene of accretion (Wakita et al., 1994). Mid-ocean formation of the Cretaceous age was transported to the accretionary zone by oceanic plate movement, scrapped, and formed the tectonic mélange. Due to the tectonic mélange in Luk Ulo, the region has considered the boundary of Java subduction during Cretaceous to Paleocene (Wakita, 2000; Hall, 2012; Clements et al., 2009; Parkinson et al., 1998; Asikin, 1974). The subduction process ceased due to the Gondwana microcontinent's collision at the edge of east and southeast Sundaland in Late Cretaceous (Smyth et al., 2007). A newer subduction zone was initiated in the south of the previous one in Middle Eocene, followed by olistostrome formation in Late Eocene - Early Oligocene – Miocene (Harsolumakso et al., 2006; Prasetyadi et al., 2006).

A second group of mélange in the area is a younger olistostrome or a sedimentary mélange, which is a gravitational sliding product in front of the accretionary wedges (Raymond, 2019; Festa et al., 2010). The olistostrome mélange in Karangsambung consists of Karangsambung and Totogan Formation, which were formed by assemblages of sandstone, limestone, conglomerate, and basaltic rocks (Prasetyadi et al., 2005). The nanoplankton and forams analysis from Karangsambung Formation indicate Middle Eocene to Late Eocene (Putra & Praptisih, 2020; Kapid & Harsolumakso, 1996; Paltrinieri et al., 1976; Asikin, 1974) and from Totogan Formation indicate Late Eocene to Early Miocene (Kapid & Harsolumakso, 1996; Soeria-Atmadja et al., 1994). Dakah and Mount Parang outcrops were observed as intrusion basalt-diabase surrounded by scaly clay of the Karangsambung and Totogan Formations (Figure 2). Setiawan et al. (2011) have a comprehensive study of Dakah-Mount Parang volcanic. Photomicrographs of samples from Dakah volcanic indicated that the major mineral is plagioclase of labradorite type albitization process. They were suggested as spilite products of low-grade metamorphism and commonly developed in a submarine environment. One of the secondary mineral presents is natrolite, indicating that the rock has experienced an alteration in a submarine condition. The whole-rock K-Ar dating of two samples of volcanic rocks cut through the Karangsambung Formation indicates the absolute age of 39.9 and 37.5 Ma, and one sample of volcanic rock in the Totogan Formation suggests the age of 26.5 Ma (Soeria-Atmadja et al., 1994).

3. METHOD

The basic principle of resistivity measurement is to inject the electric current through two electrodes and then measure the potential differences at two potential electrodes. Based on the potential difference and the injected current, we obtained apparent resistivity. The apparent resistivity can be observed as the weighted average of assumed homogeneous subsurface under the four electrodes (Milsom, 2003; Okpoli, 2013). The apparent resistivity as the function of distance qualitatively gives information on the resistivity at the designated point as the function of the depth (Milsom, 2003; Telford et al., 1990).

We used the SuperSting R8/IP and applied dipole-dipole electrode arrays. In this technique, a pair of current electrodes (I), and a pair of potential electrodes (V), were positioned on the ground in a straight (as straight as possible) line (Figure 3). The space between each pair of electrodes (***a***) should be equal. And the distance between the current and potential electrodes is an integer multiple of ***a*** (Milsom, 2003). We can obtain deeper information with a wider distance between electrodes. Therefore, we arrange the spaces based on the depth of penetration we want to achieve. In each measurement, we obtained an apparent resistivity value for the point at the midpoint between two dipoles and a depth of half the distance.

During this survey, we acquired electrical resistivity data along three transects (black lines in Figure 1C): Mount Parang (KR-1801), Dakah (KR-1802), and Wagirsambeng (KR-1803). We had 56 geo-referenced electrodes with 25 m distance between electrodes, with the length of each line is about 1375 m. Electrical current between 50 mA and 1000mA was injected for about 1.2 seconds. The injected current was varied depending on the contact‟s resistance in the field.

The data set was then filtered and processed using AGI Administrator software. Inversion modeling was applied to obtain the „true‟ resistivity from the apparent resistivity. We used EarthImager 2.4.4 software, which applied the least-squares inversion (Loke & Barker, 1996). Initial screening of data was completed to eliminate outlier data and negative apparent-resistivity. The screening process is then repeated after the first inversion process based on Gaussian distribution residual parameters. From a total of

1600 datums in each line, some were eliminated. We used the smoothness method for the inversion known as the Occam inversion (Constable et al., 1987). Inversion for each line used the half-space model with the average apparent resistivity data as the initial model.

In the inversion modeling, we also deal with the sensitivity of the model. The sensitivity indicates the potential changes caused by resistivity changes in a cell (Okpoli, 2013). Interpretation of the resistivity model should acknowledge the sensitivity calculation to validate the further analysis. Ambiguity and inaccuracy are problems we have to deal with in all geophysical modeling. The accuracy of measurements depends on the instrumental and geological factors. The data obtained were processed in such that we did not do excessive refinement to avoid data corruption. Uncertainty of the model could not be avoided. Then the assessment should be that the models conform to geological reasonableness. Due to the lack of core logging data, our interpretations are based on the general geological map and previous geological studies.

Determining rocks‟ resistivity values in this study area is challenging since most of the formation here is composed of broken fragments within a matrix. Based on the geological map, we identified several types of rocks in the area: scaly clay, clay breccia, basalt-diabase, schists, basalt-chert, and volcanic breccia. According to Telford‟s resistivity table (Telford et al., 1990), basalt with high water content has a resistivity of 4 x 10^4 ohm.m and dry basalt has resistivity up to 10^7 Ohm.m. Schist has a resistivity of 20 – 10^4 ohm.m. Clay has the lowest resistivity, which is about 1 – 100 ohm.m. Diabase has relatively high resistivity, between 10^4 – 10^6 ohm.m (Nwachukwu et al., 2018). Breccia‟s resistivity is more complex since it depends on the type of rocks and the cement condition.

In a mélange complex such as in Karangsambung, we have to look at the rock layers as a composite of several types of rocks. We simplified the description by classifying the resistivity values into three groups. A low resistivity zone (the resistivity of less than 100 ohm.m) is associated with the scaly clay and clay breccia, with a minimum amount of other rocks fragments. The second group is for hundreds' resistivity value (less than 1000 but more than 100 ohm.m). The resistivity of 100 – 200 ohm.m is mostly correlated to sand, gravel, or other sedimentary rock (Telford et al., 1990). The third group is the high resistivity zone. The geological map presents several singular bodies, such as basalt-diabase, schist, and clay breccia. We consider them a mixture of the hard-rock fragments (small or large, gravel or boulder size) within the clay matrix and have the highest resistivity of about 1000 ohm.m or higher.

4. RESULTS

4.1. Electrical Resistivity Survey

Electrical resistivity measurements were conducted at 3 locations with different surface geology (outcrop) characteristics, within the SW-NE trend of Diabase-Basalt outcrops. Line KR-1801 at Mount Parang crossed two volcanic bodies of Basalt-Diabase. The second line (KR-1802) at Dakah was in a clay-breccia environment and a relatively smaller diabase outcrop. And the third line (KR-1803) at Wagirsambeng was in the continuation of the volcanic unit trend but had basalt-chert outcrop instead of the diabase.

One indication of a good and clean data is to have the contact resistance as lowest as possible. The electrode‟s contact resistance along the Line KR-1801 generally is less than 1500 Ohms. However, at the north end of the line (first ten electrodes from point 0), the contact resistance is between 1500 and 7500 Ohm. Those electrodes with the highest contact resistance were in the metamorphic rock area. Line KR-1802 has relatively the best contact resistance, which is less than 400 Ohm. Some datums involving electrodes at 600 – 1200 m from north indicates the contact resistance between 400 and 700 Ohms. The contact resistances along the Line KR-1803 are less than 1000 Ohm. But the eight datums at the south end have a contact resistance of 3000 – 4000 Ohm.

The distribution of datums used in the inversion modeling can be seen as black dots in Figure 4(A), Figure 5(A), and Figure 6(A). Figure 4 (B), 5(B), and 6(B) display the inverted resistivity for Line KR-1801, KR-1802, and KR-1803, respectively. Iteration less than ten were required to reach convergences. A few data should be edited to minimize the misfit. The RMS errors are about 3% for all sections. The three inversion models of the resistivity, in general, display that the shallow subsurface of this area is dominated by low anomalies (blue shades in Figures 3, 4, 5). Several high anomalies bodies appear sporadically at the near surface (less than 100 m).

The last images in Figure 4(C), 5(C), and 6(C) are the survey line's sensitivity results. In analyzing the sensitivity, we focused on the distribution of sensitivity throughout the subsurface rather than the absolute value (Furman et al., 2003). Generally, near-surface sensitivity is the highest, and it is decreasing to depth. It is a normal characteristic of the sensitivity for any resistivity modeling. The cells near the surfaces received more electrical signals than the ones at the deeper depth. Therefore, they have more data in a cell to obtain higher sensitivity. In this Karangsambung electrical survey study, the sensitivity values are not all evenly distributed. In the KR-1801, the sensitivity value at the surface in the north is high, but in the south is in a medium range. Half depth of the model has a medium value on sensitivity. In the KR-1802 model, the sensitivity value at the surface is low in the north and high in the south. But only one-third of the model has a medium to high sensitivity value. A similar pattern appears in the KR-1803 model, with the distribution of the high sensitivity value is only in a very thin layer.

4.2. Resistivity Models

Figure 7 displays the resistivity model of Line KR-1801 from Mount Parang. There are two wide clusters of high resistivity at about 0 – 250 km and 750 - 1100 m (from point 0 or north-end at the left of the figure). Both appear from the surface to the depth of about 100 m. The high resistive body at the north must represent the schists, which present as the outcrop. There are several small clusters of high resistivity (yellow areas) near all surfaces, except at the 150 m south-end line. Those clusters of high resistivity bodies are the area of the basalt-diabase outcrop on the surface. The low anomaly layers surround the largest high resistive body (red cluster at about 750 – 1100 meters from point 0 and at a depth of about 50 meters). The thickness of this high resistive body is about 100 meters. This body, which has the biggest volume and highest resistivity value of all models, can be interpreted as the diabase-basalt boulders within the scaly clay layer. At the south end, a very thick low resistivity (mostly blue) appears from the surface to the bottom of the model (~300 m thickness). The low resistivity also dominated the middle part of the line (at 450 – 600 km from the north-end), where the low resistivity appears from top to bottom. Those low resistivity bodies might represent the scaly clay, which is dominated the area. The north part of the section is dominated by hundreds value of resistivity (yellow-green, ~ 100 – 500 ohm.m) with small cluster of highest resistivity (orange-red color), which corresponds well with the schist and basalt diabase outcrop. Although the solid volcanic rock body appeared small, the relatively high resistivity of this part might indicate high volcanic content.

The N-S track of Line KR-1802 in Dakah is from low to high topography, as we can see on the profile (Figure 8). This line's subsurface is dominated by low resistivity bodies (blue-green, < 50 Ohm.m), which can be correlated to the scaly clay of Karangsambung/Totogan Formation. Smaller than the previous line, some clusters of high resistivity appear near the surface. The thicknesses of these clusters are about 50 meters or less. Their presences correspond well to the geological observation that found diabase-basalt outcrop and some volcanic breccia in Dakah area (Setiawan et al., 2011). A larger high resistivity body appears in 50-meter depth at about 700 – 1000 m from the north. This body is located beneath a thin layer of low resistivity and has about 300 meters of wide and 100 meters of thickness. This high resistive body is situated almost at about the same depth as the one in KR-1801 (Mount Parang), but with a lower resistivity value. Nevertheless, we might take it as the hard-rock boulder. Beneath this body, we have a low value of resistivity (green, ~10 – 50 ohm.m). This column could represent the sedimentary environment. One particular feature in this profile is the column of low resistivity (blue, less than 5 Ohm.m) in the middle, representing a structure separated north and south.

Unlike the other two tracks, Line KR-1803 (Figure 9) in Wagirsambeng crossed an outcrop of basalt-chert. The geological observation indicated a scaly clay-dominated environment, with basalt and chert at south end of the line. The subsurface resistivity model also showed a sedimentary environment based on its low resistivity dominance (blue and green). The highest resistivity at the surface of the south end corresponds to the basalt-chert outcrop. The thickness of this body is about 50 – 100 meters. There is another large high resistive body beneath the highest part of the hill at a depth of about 50 m with about 50 m of thickness. The average resistivity value is less than 100 Ohm.m (green). Layering at the north part of the track might represent layers of scaly clay and matrixes with hard rocks fragments, which is indicated by the higher resistivity than clay supposed to have. In this section, there is also a low column of the lowest resistivity in the middle of the line (~ 600 km from the north), which might suggest a presence of a fault that separated north and south part.

5. DISCUSSION

Common studies of volcanic rocks are geochemical and dating analysis, which would suggest the age and the origin of the magmatic source. An intricate deduction aroused in relating the magmatic occurrence in a certain stage of the tectonic evolution. It is especially challenging if the volcanic rocks in questions were found in small amounts but distributed too sporadically, such as the case of basalt-diabase in Karangsambung-Totogan Formations. Generally, volcanic rock is younger than the sediment layers around due to magmatic intrusion through the existing sedimentary deposition. In an olistostrome complex, the sequences could not be that simple due to extreme disturbance of layers (Ogata et al., 2019). These volcanic rocks of basalt-diabase are distributed in an ENE-WSW trend (see Figure 1). The whole-rock K-Ar datings of those basalt-diabase rocks are 39.9 Ma, 37.5 Ma, and 26.5 Ma (Soeria-Atmadja et al., 1994). The columnar joints of basalt-diabase in Mount Parang and Dakah were observed as shallow intrusions by the surface geological mapping, and they were interpreted as necks or dikes (Setiawan et al., 2011). Karangsambung and Totogan Formations are both olistostrome formations (Asikin, 1974; Paltrinieri et al., 1976), and relative dating indicated that the rocks in Karangsambung and Totogan Formations are from Middle Eocene to Early Miocene (Putra & Praptisih, 2020; Kapid & Harsolumakso, 1996; Soeria-Atmadja et al., 1994; Paltrinieri et al., 1976; Asikin, 1974). Our resistivity models suggest that the volcanic rocks are surrounded by sedimentary deposition, including the layer beneath them, which is mostly scaly clay if we referred to the geological map. The depths (or thickness) of the volcanic rocks do not signify the deep-rooted intrusion.

Based on our current subsurface images, it is difficult to ascertain which process is responsible for the presence of volcanic bodies. The result contradicts the theory of Dakah as the center of the volcanism (Setiawan et al., 2011), and the idea of an intrusion in Mount Parang (Kamtono, 1995). The resistivity model agrees with Laesanpura et al. (2017), who suggested the sill nature of the volcanic rock due to the discontinuity to the depth. However, we prefer the non-in-situ origin of the volcanic bodies because of their singularity and relatively small characteristics. The dimension of the rocks also indicated that they are not sills in their original forms.

As products of extensive tectonic activities of the area, there are several probabilities of occurrences. Three scenarios of the origin of scattered volcanic rocks are summarized in Figure 10. The first sketch (Figure 10 A) shows the volcanic rocks as part of a sill or a dike or any intrusion body. The intrusion cut through the olistostrome formations, such as occurred in Tianshan, where olistostrome formation intruded by gabbro-diabase dike (Shu et al., 2011). If the volcanic body is interpreted as a sill, this should be part of the Eocene-Oligocene magmatic arc. The Jatibarang volcanic of Eocene (78.9 – 29.0 Ma) (Martodjojo, 1984; Soeria-Atmadja & Noeradi, 2005) could be an example of the product of the Eocene-Oligocene magmatic arc further in the West Java. Nevertheless, correlating both volcanic episodes is unfeasible since there is a lack of continuity between them. Furthermore, the appearance of a solitary body of the sill could be due to a highly intense deformation after the formation of the sill, which might occur during the Middle Miocene or younger. During that time, a tectonic phase involving major thrusting was observed almost along the south of Java and caused displacement of most Early Cenozoic volcanic rocks about 50 km northwards (Clements et al., 2009). In Dakah and Mount Parang, the thrusts might be responsible for breaking the continuation, so the upper parts are the ones that can be observed in our study. Apparently, most parts of volcanic and any layers overlain had been removed by erosion.

The second scenario (Figure 10 B) shows the volcanic boulders as small solitary bodies embedded in a scaly clay matrix. The deformation responsible for the formation should be younger than the age of volcanic, which corresponds well to the identified age. We deduced that there was a magmatic arc in the south of Java during that period (20 – 30 Ma or Late Eocene – Early Oligocene) (Soeria-Atmadja & Noeradi, 2005). Volcanic rocks developed during that time, then later sediment depositions settled on the top. Gravity sliding that caused the olistostrome formation occurred afterward during Oligocene-Early Miocene (Harsolumakso, 1999). The sliding process might also cause the disintegration of volcanic rocks.

The third possibility of the presence of the basalt-diabase boulder within the Totogan-Karangsambung formation is due to mud diapirism activity (Figure 10 C). The distinct ENE-WSW lineament of localized basalt-diabase might indicate mud diapirism. Similar observations were proposed for the occurrence of mud diapirism that might cause the presence of mélanges in small islands at the west of Sumatra (Barber et al., 2005; Barber et al., 1986; Samuel et al., 1997) and Timor (Barber, 2013; Barber et al., 1986). Remnants of intrusive volcanic were exhumed by the process of mud diapirism. This scenario might explain how the older volcanic rocks present in, the younger olistostrom sedimentary environment. A particular kind of active mud volcanoes in the olistostrom environment occurs in Mediterranean (Camerlenghi & Pini, 2009).

The volcanic rocks' origin is significant in understanding the evolution of the magmatic arc. A further detailed subsurface investigation is needed to clarify the origin of volcanic bodies within the mélange complex to understand the geodynamic process of the paleo-subduction system in this such active convergent margin.

CONCLUSION

We obtained the electric resistivity imaging along a path of the volcanic outcrop to find the evidence of the source of Oligocene volcanic activity that might occur after the formation of the mélange-olistostrome complex. The olistostrome's complex nature, where the volcanic fragments mixed within the clay matrix, caused the interpretation of models is more challenging. The modeling results confirm that all the high resistivity bodies are floating on the sedimentary layer. Any sign of continuation to the depth is not reliable. Therefore, we suggest that the volcanic rocks in Dakah and Mount Parang are part of non in situ sills, with the thicknesses of no more than 100 meters. Their nature as broken parts within the clay matrix might indicate that the volcanic had been transported from the original source.

REFERENCES

Asikin, S. (1974). *Geological evolution of Central Java from the new tectonic theory perspective (in Indonesian)*. Institut Teknologi Bandung.

Asikin, S., Handoyo, A. H., Busono, H., & Gafoer, S. (1992). *Geologic map of Kebumen Quadrangle; Java. Scale 1:100; 000*.

Barber, A. J. (2013). The origin of mélanges: Cautionary tales from Indonesia. *Journal of Asian Earth Sciences*, *76*, 428–438. https://doi.org/10.1016/j.jseaes.2012.12.021

Barber, A. J., Crow, M. J., & Milsom, J. S. (2005). *Sumatra*. London: The Geological Society.

Barber, A. J., Tjokrosapoetro, S., & Charlton, T. R. (1986). Mud Volcanoes, shale diapirs, wrench faults, and melanges in accretionary complexes, Eastern Indonesia. *The American Association of Petroleum Geologists Bulletin*, *70*(11), 1729–1741.

Barde-cabusson, S., Bolós, X., Pedrazzi, D., Lovera, R., Serra, G., Martí, J., & Casas, A. (2013). Electrical resistivity tomography revealing the internal structure of monogenetic volcanoes. *Geophysical Research Letters*, *40*, 2544–2549. https://doi.org/10.1002/grl.50538

Blaikie, T. N., Ailleres, L., Betts, P. G., & Cas, R. A. F. (2014). A geophysical comparison of the diatremes of simple and complex maar volcanoes, Newer Volcanics Province, South-Eastern Australia. *Journal of Volcanology and Geothermal Research*, *276*, 64–81.

Camerlenghi, A. N., & Pini, G. A. (2009). Mud volcanoes, olistostromes and argille scagliose in the Mediterranean region. *Sedimentologi*, *56*, 319–365. https://doi.org/10.1111/j.1365-3091.2008.01016.x

Clements, B., Hall, R., Smyth, H. R., & Cottam, M. A. (2009). Thrusting of a volcanic arc: a new structural model for Java. *Petroleum Geoscience*, *15*(2), 159–174. https://doi.org/10.1144/1354-079309-831

Constable, S. C., Parker, R. L., & Constable, G. C. (1987). Occam‟s inversion: A practical algorithm for generating smooth models from electromagnetic sounding data. *Geophysics*, *52*(3), 289–300.

Festa, A., Pini, G. A., Dilek, Y., & Codegone, G. (2010). Melanges and melange-forming prcesses: a historical overview and new concepts. *International Geology Review*, *52*(10–12), 1040–1105.

Fitterman, D. V, Stanley, W. D., & Bisdorf, R. J. (1988). Electrical structure of Newberry Volcano, Oregon. *Journal of Geophysical Research: Solid Earth*, *93*(B9), 10119–10134.

Haberland, C., Bohm, M., & Asch, G. (2014). Accretionary nature of the crust of Central and East Java (Indonesia) revealed by local earthquake travel-time tomography. *Journal of Asian Earth Sciences*, *96*, 287–295. https://doi.org/10.1016/j.jseaes.2014.09.019

Hall, R. (2012). Late Jurassic–Cenozoic reconstructions of the Indonesian region and the Indian Ocean. *Tectonophysics*, *570–571*, 1–41. https://doi.org/10.1016/j.tecto.2012.04.021

Harsolumakso, A H, Sapiie, B., Tuakia, Z., & Yudha, R. I. (2016). Luk Ulo Melange Complex, Central Java, Indonesia; Characteristics , Origin and Tectonic significance. In *Asia Oceania Geoscience Society Conference*. https://doi.org/10.13140/RG.2.2.14457.26728

Harsolumakso, Agus Handoyo. (1996). Olistostrome in Luk Ulo, Central Java; a review of stratigraphy, age and deformation (in Indonesian). In *Proceeding of National Seminar in The role of geological resources in the long term development of Indonesia* (pp. 101–121).

Harsolumakso, Agus Handoyo. (1999). Diabase in Karangsambung, Luk Ulo, Central Java: Is the basaltic group an intrusive body? (In Indonesian). In *Proceeding of National Seminar in Geological Resources. Geological Engineering, University of Gadjah Mada.* (pp. 1–6). Yogyakarta: Geology Department, Universitas Gajah Mada.

Harsolumakso, Agus Handoyo, Sapiie, B., & Suparka, E. (2006). The Luk Ulo-Karangsambung Complex of Central Java; from Subduction to Collisional Tectonics. In *Proceedings Persidangan Bersama UKM-ITB*.

Ingham, M. (2005). Deep electrical structure of the Central Volcanic Region and Taupo Volcanic Zone , New Zealand. *Earth Planets Space*, *57*, 591–603.

Junaid, M., Abdullah, R. A., Saa, R., Alel, M., Ali, W., & Ullah, A. (2019). Recognition of boulder in granite deposit using integrated borehole and 2D electrical resistivity imaging for effective mine planning and development. *Bulletin of the Geological Society of Malaysia*, *67*(June), 99–104.

Kadarusman, A., Massonne, H., Roermund, H. Van, Permana, H., & Munasri. (2007). P-T Evolution of Eclogites and Blueschists from the Luk Ulo Complex of Central Java, Indonesia P-T Evolution of Eclogites and Blueschists. *International Geology Review*, *49*, 329–356. https://doi.org/10.2747/0020-6814.49.4.329

Kamtono. (1995). *Interpretation of 2D gravity profiles and its implication to the origin of melange's blocks in Luk Ulo, Karangsambung, Central Java (in Indonesian)*. Geological Engineering Department, Institute Teknologi Bandung.

Kapid, R., & Harsolumakso, A. H. (1996). Nannoplankton Study of Karangsambung and Totogan Formation in Luk Ulo, Kebumen, Java (in Indonesian). *Bul. Geol*, *26*, 45–54.

Laesanpura, A., Dahrin, D., & Sugianto, A. (2017). AMT and gravity across praTertiary rock complex of Kebumen, Central Java, Indonesia. In *AIP Conference Proceeding 1st International Geo-Electromagnetic Workshop (Geo-EM)* (Vol. 1861, pp. 030029.1-030029.4). https://doi.org/10.1063/1.4990916

Loke, M. H., & Barker, R. D. (1996). Rapid least-squares inversion of apparent resistivity pseudosections using a Quasi-Newton method. *Geophysical Prospeecting*, *44*, 131–152. https://doi.org/10.1111/j.1365-2478.1996.tb00142.x

Martodjojo, S. (1984). *Evolution of Bogor Basin, West Java*. Institut Teknologi Bandung.

Milsom, J. (2003). *Field Geophysics* (Third). West Sussex, England: John Wiley & Sons Ltd.

Miyazaki, K., Sopaheluwakan, J., Zulkarnain, I., & Wakita, K. (1998). A jadeite - quartz - glaucophane rock from Karangsambung, Central Java, Indonesia. *The Island Arc*, 7, 223–230.

Nwachukwu, M. A., Nwosu, L. I., Uzoije, P. A., & Nwoko, C. A. (2018). 1D resistivity inversion technique in the mapping of igneous intrusives ; A step to sustainable quarry development. *Journal of Sustainable Mining*, *16*(4), 127–138. https://doi.org/10.1016/j.jsm.2017.11.001

Ogata, K., Festa, A., Pini, G. A., Poga, Ž., & Lucente, C. C. (2019). Substrate deformation and incorporation in sedimentary mélanges (olistostromes): Examples from the northern Apennines (Italy) and northwestern Dinarides (Slovenia). *Gindwana Research*, *74*, 101–125. https://doi.org/10.1016/j.gr.2019.03.001

Ogawa, Y., Matsushima, N., Oshima, H., Takakura, S., Utsugi, M., Hirano, K., … Doi, T. (1998). A resistivity cross-section of Usu Volcano, Hokkaido, Japan, by audiomagnetotelluric soundings. *Earth, Planets and Space*, *50*(4), 339–346.

Okpoli, C. C. (2013). Sensitivity and resolution capacity of electrode configurations. *International Journal of Geophysics*, *2013*, 608037. https://doi.org/10.1155/2013/608037

Paltrinieri, F., Sajekti, S., & Suminta. (1976). Biostratigraphy of the Jatibungkus section (Lokulo area) in Central Java. In *Proceedings Indonesian Petroleum Association Annual Convention* (pp. 195–204).

Parkinson, C. D., Miyazaki, K., Wakita, K., Barber, A. J., & Carswell, D. A. (1998). An overview and tectonic synthesis of the pre-Tertiary very-high-pressure metamorphic and associated rocks of Java, Sulawesi and Kalimantan, Indonesia. *Island Arc*, *7*(1–2), 184–200. https://doi.org/10.1046/j.1440-1738.1998.00184.x

Prasetyadi, C., Suparka, E. M., Harsolumakso, A. H., & Sapiie, B. (2005). Eastern Java basement rock study: Preliminary results of recent field study in Karangsambung and Bayat areas. In *Proceedings Joint Convention Surabaya 2005-HAGI-IAGI-PERHAPI* (pp. 310–321).

Prasetyadi, C., Suparka, E. R., Harsolumakso, A. H., & Sapiie, B. (2006). An overview of Paleogene stratigraphy of the Karangsambung area, central Java: Discovery of a new type of Eocene rock. In *Proceedings of Jakarta 2006 International Geosciences Conference and Exhibition* (pp. 3–6). Jakarta.

Putra, P. S., & Praptisih. (2020). Olisostrome source sedimentary rocks relative age of the Karangsambung Formation, Kebumen, Central Java. *Journal of Geology and Mineral Resources*, *21*(1), 25–31.

Raymond, L. A. (2019). Perspectives on the roles of melanges in subduction accretionary complexes : A review. *Gondwana Research*, *74*, 68–89. https://doi.org/10.1016/j.gr.2019.03.005

Samuel, M. A., Harbury, N. A., Bakri, A., Banner, F. T., & Hartono, L. (1997). A new stratigraphy for the islands of the Sumatran Forearc , Indonesia. *Journal of Asian Earth Sciences*, *15*(4), 339–380.

Setiawan, N. I., Yuwono, Y. S., & Sucipta, I. G. B. E. (2011). The Genesis of Tertiary “Dakah Volcanics” in Karangsambung, Kebumen, Central Java. *Majalah Geologi Indonesia*, *26*(1), 29–44.

Shu, L., Wang, B., Zhu, W., Guo, Z., Charvet, J., & Zhang, Y. (2011). Timing of initiation of extension in the Tianshan, based on structural, geochemical and geochronological analyses of bimodal volcanism and olistostrome in the Bogda Shan (NW China). *International Journal of Earth Science*, *100*, 1647–1663. https://doi.org/10.1007/s00531-010-0575-5

Smyth, H. R., Hamilton, P. J., Hall, R., & Kinny, P. D. (2007). The deep crust beneath island arcs : Inherited zircons reveal a Gondwana continental fragment beneath East Java , Indonesia. *Earth and Planetary Science Letters*, *258*, 269–282. https://doi.org/10.1016/j.epsl.2007.03.044

Soeria-Atmadja, R., Maury, R. C., Bellon, H., Pringgoprawiro, H., Polve, M., & Priadi, B. (1994). Tertiary magmatic belts in Java. *Journal of Southeast Asian Earth Sciences*, *9*(I/2), 13–27.

Soeria-Atmadja, R., & Noeradi, D. (2005). Distribution of Early Tertiary volcanic rocks in south Sumatra and West Java. *The Island Arc*, *14*, 679–686.

Suparka, E. (1988). *Study on petrology and geochemistry of North Karangsambung Ophiolite (in Indonesian)*. Institut Teknologi Bandung.

Telford, W. M., Geldart, L. P., & Sheriff, R. E. (1990). *Applied Geophysics* (1nd ed.). Cambridge University Press.

Troiano, A., Isaia, R., Di Giuseppe, M. G., Tramparulo, F. D. A., & Vitale, S. (2019). Deep Electrical Resistivity Tomography for a 3D picture of the most active sector of Campi Flegrei caldera. *Scientific Reports*, *9*, 15124. https://doi.org/10.1038/s41598-019-51568-0

Wakita, K. (2000). Cretaceous accretionary–collision complexes in central Indonesia.

Journal of Asian Earth Sciences, *18*, 739–749. https://doi.org/10.1016/S1367-9120(00)00020-1

Wakita, Koji, Munasri, & Widoyoko, B. (1994). Cretaceous radiolarians from the Luk-Ulo Melange Complex in the Karangsambung area, Central Java, Indonesia. *Journal of Southeast Asian Earth Sciences*, *9*(1/2), 29–43.

Yuwono, Y. S. (1997). The occurence of submarine Arc-Volcanism in the Accretionary Complex of The Luk Ulo Area, Central Java. *Bulletin Geologi*, *27*, 15–26.

FIGURE CAPTIONS

Figure 1. A. Karangsambung was located at the subduction zone, where a microplate subducted toward the Sundaland in Cretaceous (e.g. Hall, 2012; Wakita, 2000; Soeria-Atmadja et al., 1994). B. Geological map of Karangsambung Complex shows the distribution of formations. Black box is the study area. C. Geological map of study area shows rocks distribution. Black lines KR18-01 (Mount Parang), KR18-02 (Dakah), and KR18-03 (Wagirsambeng) are the resistivity survey lines. Geological map source: Harsolumakso et al. (2016).

Figure 2. Field photograph of Mount Parang, one of the Paleogene age volcanic outcrops in Karangsambung. One of the survey lines crossed the hill (on the left).

Figure 3. Sketch of electrodes configurations (*a* is the distance between two electrodes, *na* is the total distance of n electrodes). We used 56 electrodes with a = 25 m at each line of measurement.

Figure 4. Apparent resistivity result of KR18-01 (Mount Parang). From top to bottom: A. Calculated apparent resistivity pseudosection. The black dots indicate datums used in inversion modeling. B. Inverted resistivity model. This section shows a

large body of high resistivity lies on a very low resistives body. Notice that the maximum scale in this section is 10000 ohm.m. C. Relative sensitivity section. The sensitivity in general is decreasing to the depth, except a small anomaly in between 750 and 900-meters distances from point 0, the same location as the high resistivity in B.

Figure 5. Resistivity result of KR18-02 (Dakah). From top to bottom: A. Calculated apparent resistivity pseudosection. The black dots indicate datums used in inversion modeling. B. Inverted resistivity model. There are only few small bodies of high resistivity, with the highest resistivity only about 1200 ohm.m. C. Relative sensitivity section. The sensitivity discontinuity is at about the large area of relatively higher resistivity cluster.

Figure 6. Resistivity result of KR18-03 (Wagirsambeng). From top to bottom: A. Calculated apparent resistivity pseudosection. The black dots indicate datums used in inversion modeling. B. Inverted resistivity model, which indicates small variation of the resistivity values (the highest only about 450 ohm.m). C. Relative sensitivity section. The sensitivity distribution is almost normal in all part of section, where the value is decreasing to the depth.

Figure 7. Resistivity model of KR18-01 (Mount Parang). The color bar on the top indicates the geological outcrop (Sh=Schistes , Cb=clay breccia, Bd = basalt and diabase). The depth of basalt-diabase body is about 100 m, and the width is about 400-500 m. With the resistivity scale reach 10000 ohm.m, the high resistive body is more prominent than the ones in the other sections.

Figure 8. Resistivity model of KR18-02 (Dakah). The color bar on the top indicates the

geological outcrop (Cb=clay breccia, Bd = basalt and diabas, Vb=volcanic breccia). The basalt-diabase bodies at the surface are distributed in some distances. But there is one relatively larger high resistivity body to the depth of 100 meter.

Figure 9. Resistivity model of KR18-03 (Wagirsambeng). The color bar on the top indicates the geological outcrop (Sc=scaly clay, Bc = basalt and cherts). The high resistive bodies in this section represent the basalt-cherts, which has about 100 m thickness at the south edge of the section.

Figure 10. Three hypothetical origins of the volcanic rocks in Dakah – Mount Parang. A. Intrusions of volcanic rocks, which had been broken apart due to structural forces (faults). Faults are parts of deformation in Neogene time. B. Exotic blocks of volcanic rocks as parts of landslide masses that formed the olistostrome. Faults are parts of deformation in Neogene time. C. Exhumation of volcanic rocks by mud diapirism. The southward faults in the bottom layer are the products of Paleogen deformation related to previous subduction.

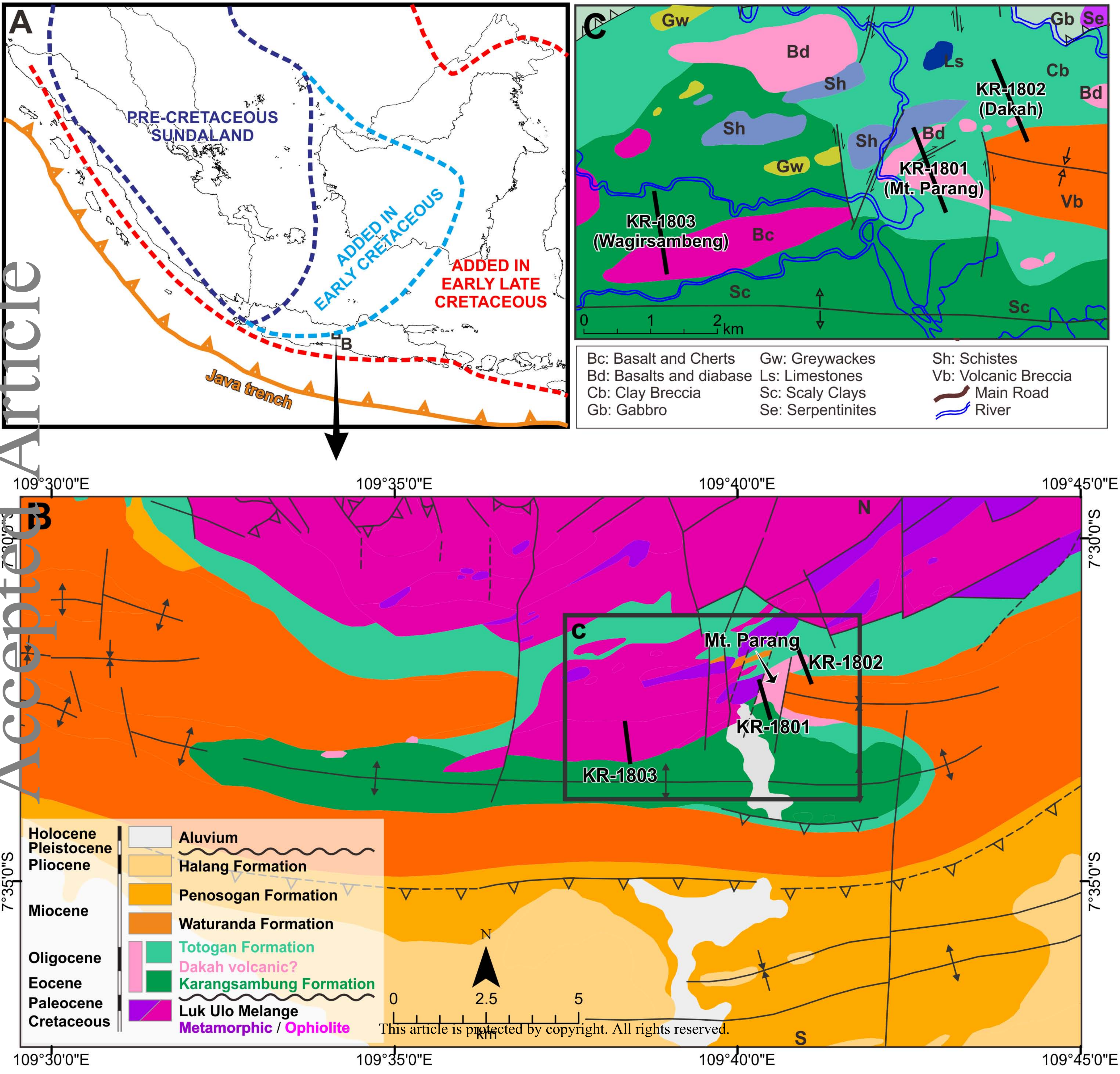
A
PRE-CRETACEOUS SUNDALAND
ADDED IN EARLY CRETACEOUS
ADDED IN EARLY LATE CRETACEOUS
Java trench
B
C
Gw
Bd
Sh
Ls
Cb
Gb
Se
KR-1802 (Dakah)
KR-1801 (Mt. Parang)
KR-1803 (Wagirsambeng)
Bc
Vb
Sc
0 1 2 km
Bc: Basalt and Cherts
Bd: Basalts and diabase
Cb: Clay Breccia
Gb: Gabbro
Gw: Greywackes
Ls: Limestones
Sc: Scaly Clays
Se: Serpentinites
Sh: Schistes
Vb: Volcanic Breccia
Main Road
River
109°30'0"E
109°35'0"E
109°40'0"E
109°45'0"E
7°30'0"S
7°35'0"S
N
S
Mt. Parang
KR-1802
KR-1801
KR-1803
Holocene
Pleistocene
Pliocene
Miocene
Oligocene
Eocene
Paleocene
Cretaceous
Aluvium
Halang Formation
Penosogan Formation
Waturanda Formation
Totogan Formation
Dakah volcanic?
Karangsambung Formation
Luk Ulo Melange
Metamorphic / Ophiolite
0 2.5 5
km


Basalt Diabase

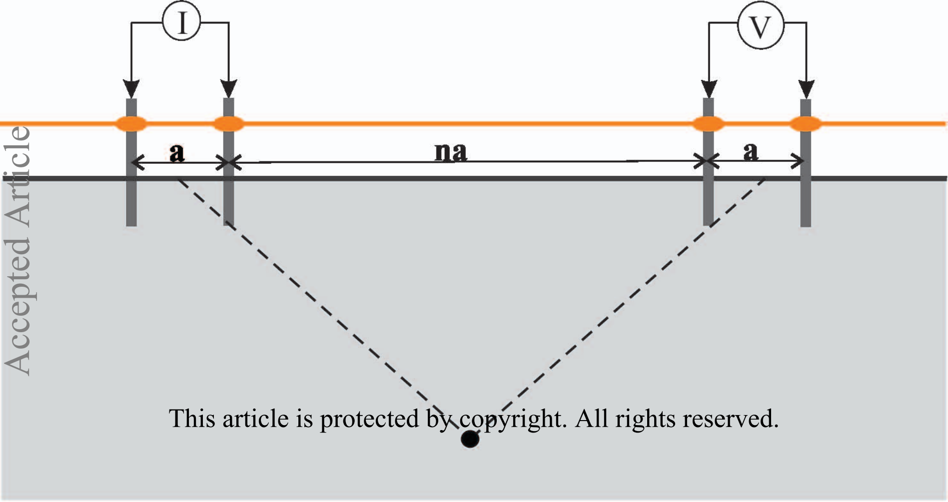
I
V
a
na
a

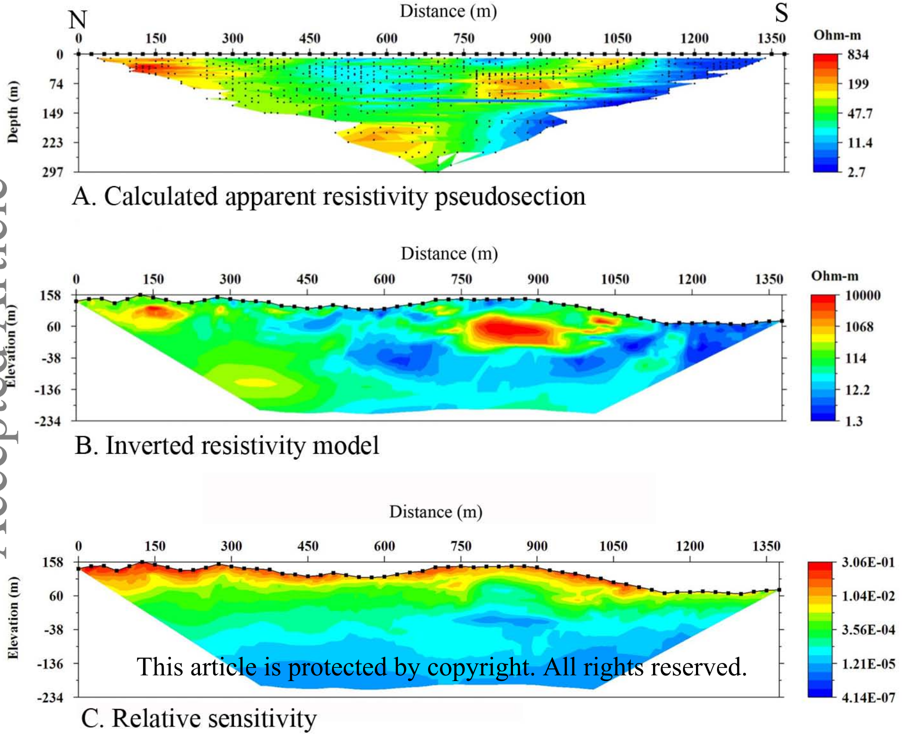
N
S
Distance (m)
0
150
300
450
600
750
900
1050
1200
1350
Depth (m)
0
74
149
223
297
Ohm-m
834
199
47.7
11.4
2.7
A. Calculated apparent resistivity pseudosection
Distance (m)
Elevation (m)
158
60
-38
-136
-234
Ohm-m
10000
1068
114
12.2
1.3
B. Inverted resistivity model
Distance (m)
Elevation (m)
3.06E-01
1.04E-02
3.56E-04
1.21E-05
4.14E-07
C. Relative sensitivity

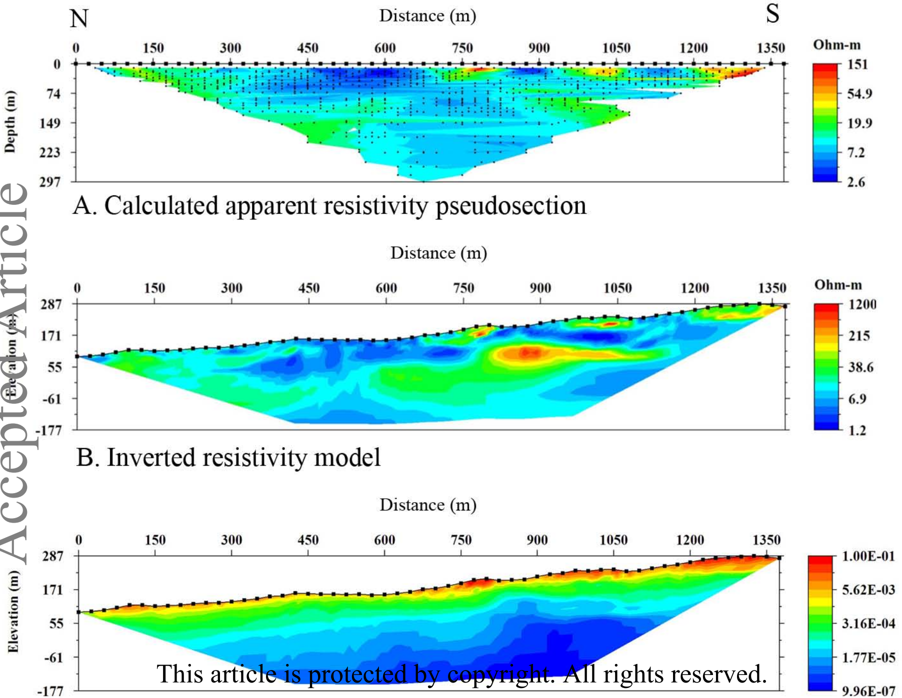

A. Calculated apparent resistivity pseudosection

B. Inverted resistivity model

C. Relative sensitivity

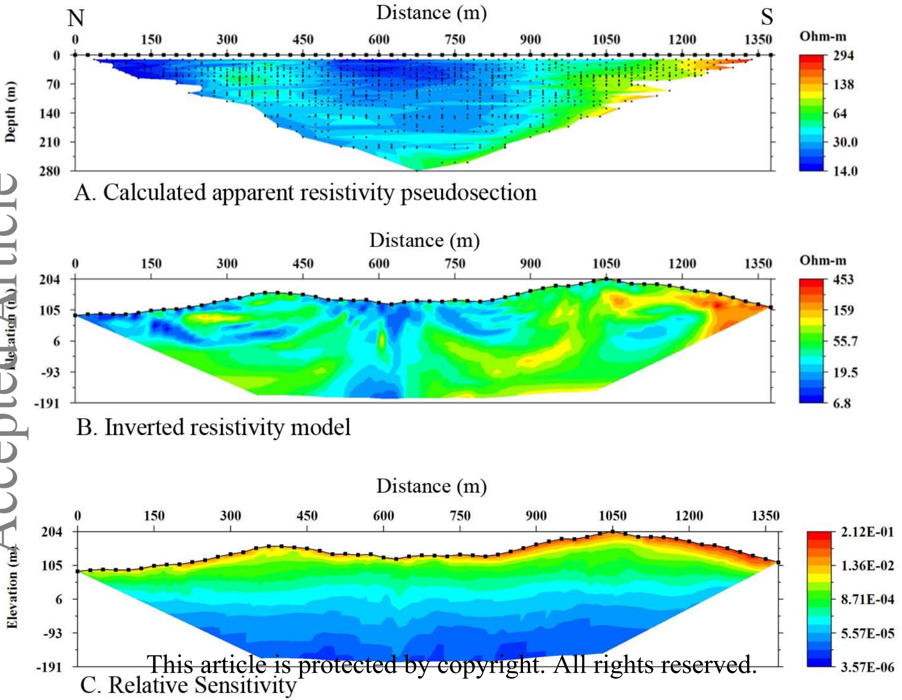
N
S
Distance (m)
0
150
300
450
600
750
900
1050
1200
1350
Depth (m)
0
70
140
210
280
Ohm-m
294
138
64
30.0
14.0
A. Calculated apparent resistivity pseudosection
Distance (m)
Elevation (m)
204
105
6
-93
-191
Ohm-m
453
159
55.7
19.5
6.8
B. Inverted resistivity model
Distance (m)
Elevation (m)
2.12E-01
1.36E-02
8.71E-04
5.57E-05
3.57E-06
C. Relative Sensitivity

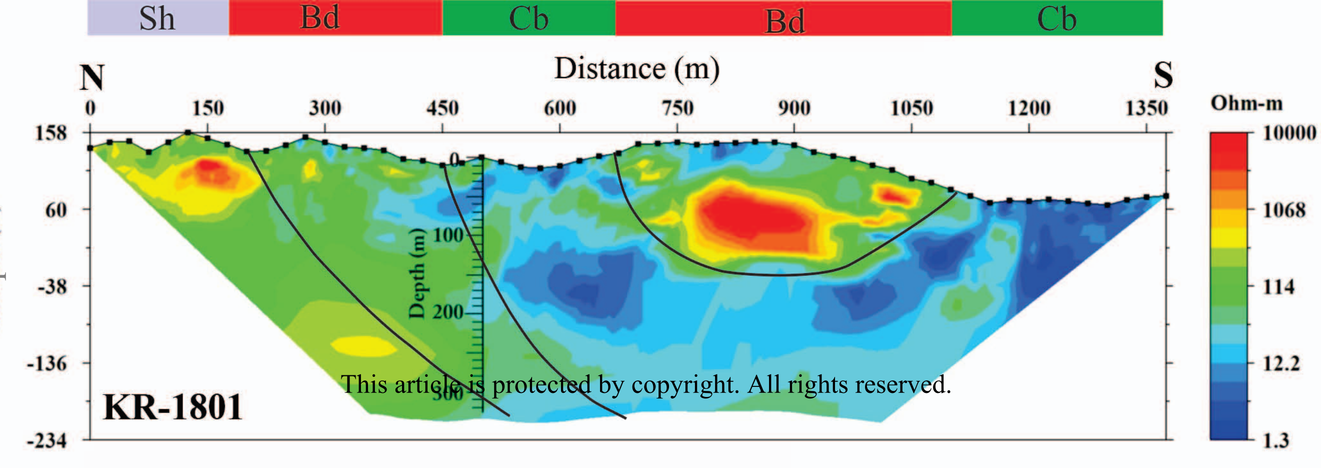
Sh
Bd
Cb
Bd
Cb
Distance (m)
N
S
0
150
300
450
600
750
900
1050
1200
1350
Ohm-m
10000
1068
114
12.2
1.3
158
60
-38
-136
-234
Depth (m)
0
100
200
300
KR-1801

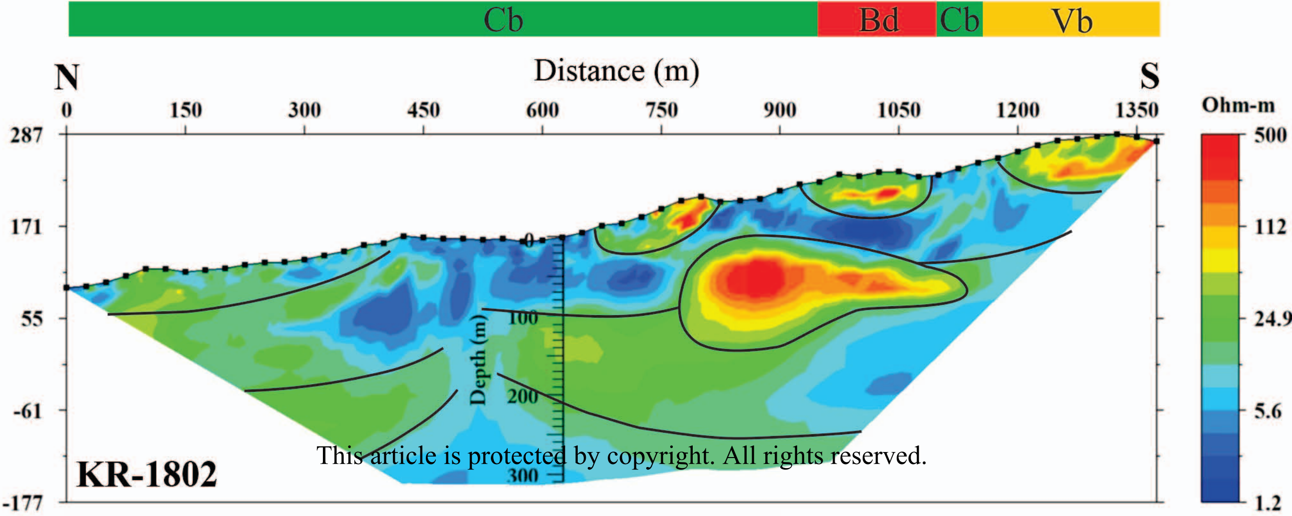
Cb
Bd
Cb
Vb
N
Distance (m)
S
0
150
300
450
600
750
900
1050
1200
1350
Ohm-m
287
171
55
-61
-177
Elevation (m)
Depth (m)
0
100
200
300
500
112
24.9
5.6
1.2
KR-1802

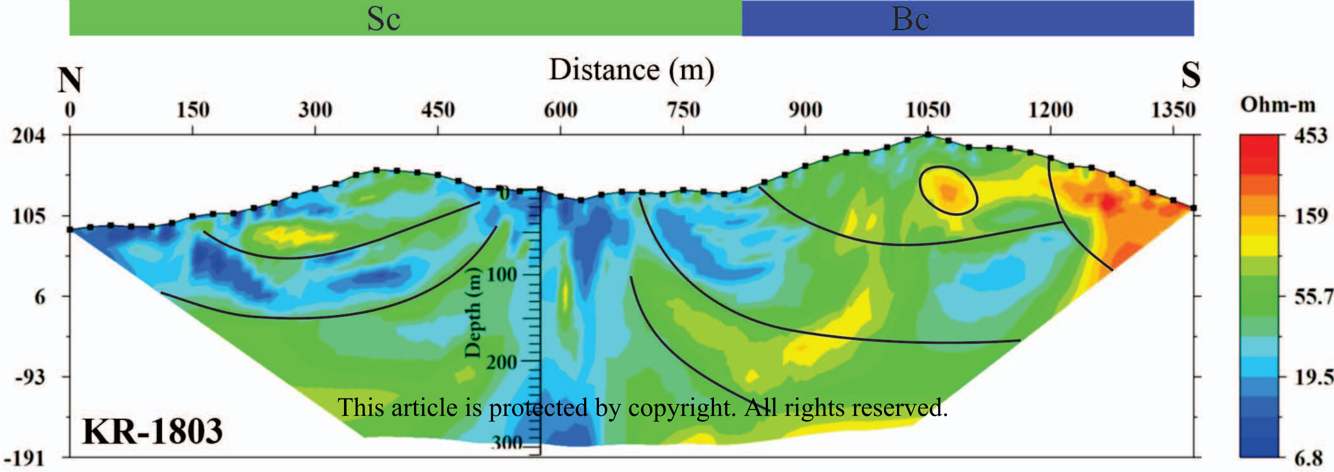
Sc
Bc
Distance (m)
N
S
0
150
300
450
600
750
900
1050
1200
1350
Ohm-m
453
159
55.7
19.5
6.8
204
105
6
-93
-191
Elevation (m)
Depth (m)
100
200
300
KR-1803

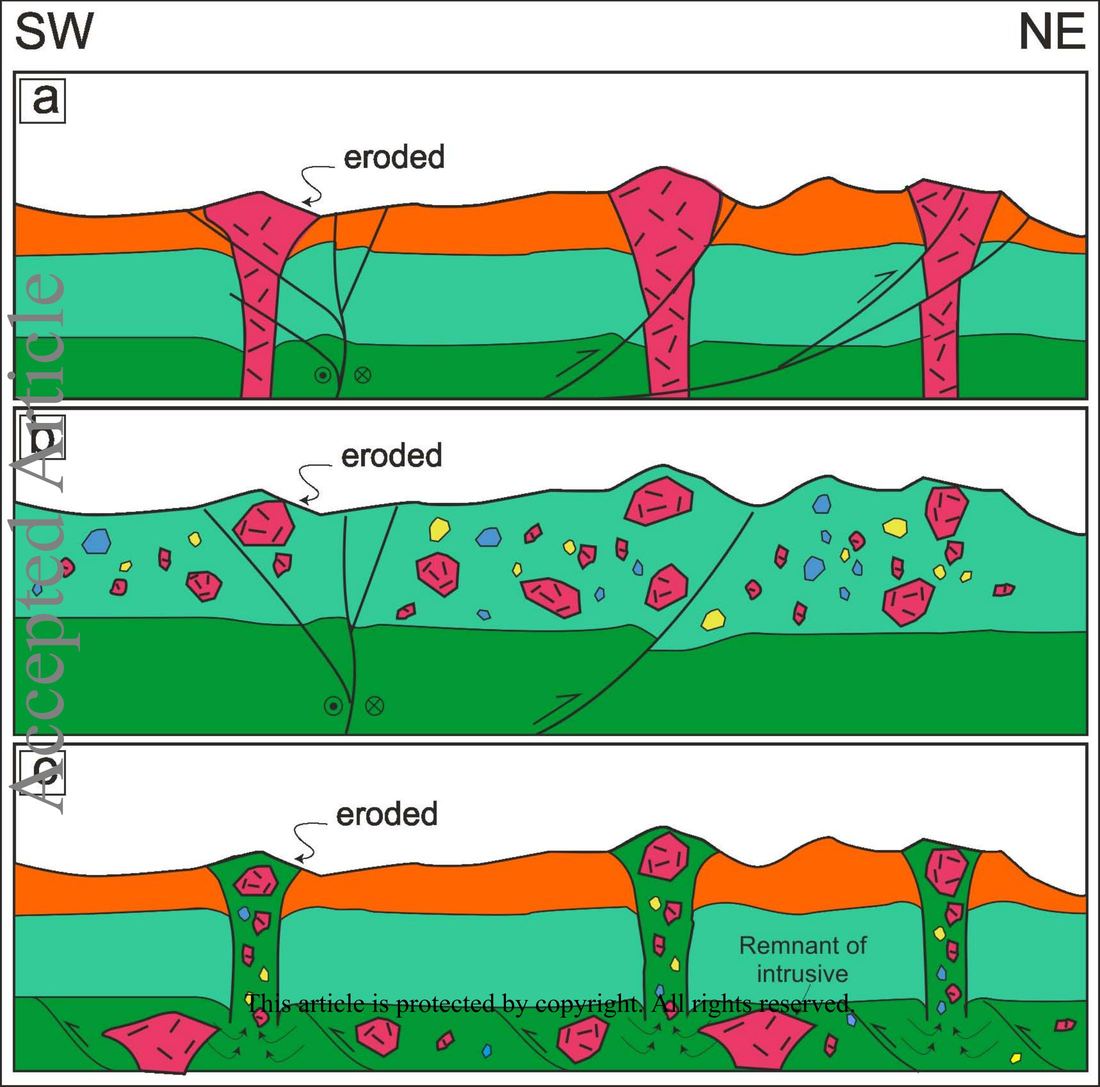
SW
NE
a
eroded
b
eroded
c
eroded
Remnant of
intrusive